Very low loss reactively ion etched Tellurium Dioxide planar rib waveguides for linear and non-linear optics

S. J. Madden*, K. T. Vu

Laser Physics Centre, Research School of Physics and Engineering, Australian National University, Canberra, ACT 0200, Australia

** sjm111@rsphysse.anu.edu.au*

Abstract: We report on the fabrication and optical properties of the first very low loss nonlinear Tellurite planar rib waveguides ever demonstrated. A new reactive ion etch process based on Hydrogen as the active species was developed to accomplish the low propagation losses. Optical losses below ~0.05dB/cm in most of the NIR spectrum and ~0.10dB/cm at 1550nm have been achieved - the lowest ever reported by more than an order of magnitude and clearly suitable for planar integrated devices. We demonstrate strong spectral broadening of 0.6ps pulses in waveguides fabricated from pure TeO_2, in good agreement with simulations.

OCIS codes: (060.4510) Optical communications; (070.4340) Nonlinear optical signal processing; (130.3120) Integrated optics devices

References and links

1. R. A. H. El-Mallawany, Tellurite Glasses Handbook: physical properties and data (CRC Press, 2002).
2. S.-H. Kim, T. Yoko, and S. Sakka, "Nonlinear Optical Properties of TeO_2-Based Glasses: MOx-TeO2 (M = Sc, Ti, V, Nb, Mo, Ta, and W) Binary Glasses," J. Am. Ceram. Soc. **76**, 2486 (1993).
3. D. A. Gaponov, and A. S. Biryukov, "Optical properties of microstructure tellurite glass fibres," Quantum Electron. **36**(4), 343–348 (2006).
4. G. Ghosh, "Sellmeier coefficients and chromatic dispersions for some tellurite glasses," J. Am. Ceram. Soc. **78**(10), 2828–2830 (1995).
5. R. Jose, and Y. Ohishi, "Enhanced Raman gain coefficients and bandwidths in P_2O_5 and WO added tellurite glasses for Raman gain media," Appl. Phys. Lett. **89**(12), 221122 (2006).
6. G. S. Murugan, T. Suzuki, and Y. Ohishi, "Phospho-tellurite glasses containing heavy metal oxides for ultrabroad band fiber Raman amplifiers," Appl. Phys. Lett. **86**(22), 221109 (2005).
7. R. Jose, and Y. Ohishi, "Ultra-broadband Raman gain media for photonics device applications," International Society for Optical Engineering, Bellingham WA, WA 98227–0010,San Jose, CA, 64690 (2007).
8. R. Jose, and Y. Ohishi, "Higher nonlinear indices, Raman gain coefficients, and bandwidths in the TeO_2 -ZnO-Nb_2O_5 -MoO_3 quaternary glass system," Appl. Phys. Lett. **90**(21), 221104 (2007).
9. R. Stegeman, C. Rivero, K. Richardson, G. Stegeman, P. Delfyett, Jr., Y. Guo, A. Pope, A. Schulte, T. Cardinal, P. Thomas, and J. C. Champarnaud-Mesjard, "Raman gain measurements of thallium-tellurium oxide glasses," Opt. Express **13**(4), 1144–1149 (2005).
10. L. Kassab, R. Pinto, R. Kobayashi, M. Piasecki, P. Bragiel, and I. Kityk, "Photoinduced second-order optical susceptibilities of Er_2O_3 doped TeO_2–GeO_2–PbO glasses," Opt. Commun. **274**(2), 461–465 (2007).
11. A. Jha, S. Shaoxiong, H. Li Hui, and P. Joshi, "Spectroscopic properties of rare earth metal ion doped tellurium oxide glasses and fibres," J. Opt. **33**, 157 (2004).
12. E. B. Intyushin, and V. A. Novikov, "Tungsten-tellurite glasses and thin films doped with rare-earth elements produced by radio frequency magnetron deposition," Thin Solid Films **516**(12), 4194–4200 (2008).
13. M. Yamada, A. Mori, K. Kobayashi, H. Ono, T. Kanamori, K. Oikawa, Y. Nishida, and Y. Ohishi, "Gain-flattened tellurite based EDFA with a flat amplification bandwidth of 76 nm," IEEE Photon. Technol. Lett. **10**(9), 1244–1246 (1998).
14. S. Shen, A. Jha, and X. Liu, M. Naftaly, K. Bindra, H. J. Bookey, and A. K. Kar, "Tellurite glasses for broadband amplifiers and integrated optics," J. Am. Ceram. Soc. **85**(6), 1391–1395 (2002).
15. S. Shen, M. Naftaly, and A. Jha, "Tm- and Er-doped tellurite glass fiber for a broadband amplifier at 1450-1600nm", Proc. SPIE, **3849**, Paper 3849–12, (1999).
16. A. Mori, H. Masuda, K. Shikano, K. Oikawa, K. Kato, and M. Shimizu, "Ultra-Wideband tellurite based Raman fibre amplifier," Electron. Lett. **37**(24), 1442–1443 (2001).
17. S. Man, E. Pun, and P. Chung, "Tellurite glass for 1.3μm optical amplifiers," Opt. Commun. **168**(5-6), 369–373 (1999).

#114691 - $15.00 USD Received 23 Jul 2009; revised 8 Sep 2009; accepted 9 Sep 2009; published 17 Sep 2009

18. H. Bookey, K. Bindra, A. Kar, and B. Wherrett, "Telluride glass fibres for all optical switching: - nonlinear optical properties and fibre characterization," in Proceedings of the 2002 IEEE/LEOS Workshop on Fibre and Passive Optical Components, 29 – 34 (2002).
19. P. Domachuk, N. A. Wolchover, M. Cronin-Golomb, A. Wang, A. K. George, C. M. B. Cordeiro, J. C. Knight, and F. G. Omenetto, "Over 4000 nm bandwidth of mid-IR supercontinuum generation in sub-centimeter segments of highly nonlinear tellurite PCFs," Opt. Express **16**(10), 7161–7168 (2008).
20. E. Chierici, M. C. Didavide, A. Moro, O. Rossotto, L. Tallone, and E. Monchiero, "Direct writing of channel waveguide on a tellurite glass using a focused ultraviolet laser beam", IEEE/LEOS Proc. Workshop Fibre Passive Components, 24–28, (2002).
21. E. Monchiero, D. Milanese, M. Ferraris, L. Tallone, and E. Chierici, "Direct writing of waveguides on tellurite glasses", ICOXIX: Optics for the Quality of life, Proc. SPIE **4829**, 161–162 (2002).
22. Y. Tokuda, M. Saito, M. Takahashi, K. Yamada, W. Watanabe, K. Itoh, and T. Yoko, "Waveguide formation in niobium tellurite glass by pico and femtosecond laser pulses," J. Non-Cryst. Solids **326**, 472–475 (2003).
23. P. Nandi, G. Jose, C. Jayakrishnan, S. Debbarma, K. Chalapathi, K. Alti, A. K. Dharmadhikari, J. A. Dharmadhikari, and D. Mathur, "Femtosecond laser written channel waveguides in tellurite glass," Opt. Express **14**(25), 12145–12150 (2006).
24. T. T. Fernandez, G. D. Valle, R. Osellame, G. Jose, N. Chiodo, A. Jha, and P. Laporta, "Active waveguides written by femtosecond laser irradiation in an erbium-doped phospho-tellurite glass," Opt. Express **16**(19), 15198–15205 (2008).
25. G. N. Conti, V. K. Tikhomirov, M. Bettinelli, S. Berneschi, M. Brenci, B. Chen, S. Pelli, A. Speghini, A. B. Seddon, and G. C. Righini, "Characterization of ion-exchanged waveguides in tungsten tellurite and zinc tellurite Er3+ doped glasses," Opt. Eng. **42**(10), 2805–2811 (2003).
26. G. N. Conti, S. Berneschi, M. Bettinelli, M. Brenci, B. Chen, S. Pelli, A. Speghini, and G. Righini, "Rare-earth doped tungsten tellurite glasses and waveguides: fabrication and characterization," J. Non-Cryst. Solids **345**, 343–348 (2004).
27. Y. Ding, S. Jiang, T. Luo, Y. Hu, and N. Peyghambarian, "Optical waveguides prepared in Er3+doped tellurite glass by Ag+-Na+ ion-exchange," Proc. SPIE **4282**, 23–30 (2001).
28. S. Berneschi, M. Brenci, G. Nunzi Conti, S. Pelli, G. C. Righini, I. Bányász, A. Watterich, N. Khanh, M. Fried, and F. Pászti, "Channel waveguide fabrication in Er3+ doped tellurite glass by ion beam irradiation", Proc. SPIE, **6475**, 647509–1 – 647509–6, (2007).
29. S. M. Pietralunga, M. Lanata, M. Ferè, D. Piccinin, G. Cusmai, M. Torregiani, and M. Martinelli, "High-contrast waveguides in sputtered pure TeO_2 glass thin films," Opt. Express **16**(26), 21662–21670 (2008).
30. R. Nayak, V. Gupta, A. L. Dawar, and K. Sreenivas, "Optical waveguiding in amorphous tellurium oxide thin films," Thin Solid Films **445**(1), 118–126 (2003).
31. R. H. Clarke, "Theory of reflection from antireflection coatings," Bell Syst. Tech. J. **62**, 2885–2891 (1983).

1. Introduction

Tellurite glasses are of considerable interest for a broad range of applications in fields such as optical telecommunications, sensing, defense, etc due to their wealth of excellent optical properties. These glasses are highly transparent from around 400nm to ~6um in the mid infra-red; have high acousto-optic figures of merit 3x that of quartz) [1]; high linear refractive indices of up to 2.2 at 1900nm [2], and low material dispersion. Pure TeO_2 has zero dispersion near 1700nm; more complex glasses have zero dispersion beyond 2000nm [3,4], and the zero dispersion point in a waveguide device can therefore easily be tuned to the telecommunication window [3]. Tellurites have large Raman shifts (up to 1200cm^{-1} in some compositions [5,6]) and large Raman gain coefficients of order of 60x silica [7-9]. Tellurites possess the largest optical nonlinearity of any oxide glass at up to 80-100x that of silica [8] and poling of tellurite glasses has also led to the largest induced second order non-linearity in any oxide glass to date [10]. Tellurite glasses are also excellent hosts for many rare earth ions such as Er^{3+}, Tm^{3+}, Ho^{3+}, Pr^{3+}, etc, displaying additional transitions not seen in silica for example at 1300nm and beyond 2000nm which are crucial for future active integrated optics components [11,12]. Furthermore, Tellurite glasses are thermally and mechanically stable.

These properties are well known and extensively exploited in the fields of accousto-optic devices, fiber based optical amplification [e.g 13-17.], and non-linear optical processing [e.g 16,18,19.]. However, planar tellurite devices have, until now, proven to be rather problematic. There have been a number of reports [20–29] of planar waveguides fabricated in tellurite glasses using techniques such as UV direct write [20,21], femtosecond laser direct write [22–24], ion exchange [25–27], ion implant [28], and sputter etching [29]. Whilst some of these methods have realized small channel waveguides, propagation losses were high (lowest

#114691 - $15.00 USD Received 23 Jul 2009; revised 8 Sep 2009; accepted 9 Sep 2009; published 17 Sep 2009

reported loss of 1.3dB/cm [24]) and there are no reports of losses even approaching 0.2dB/cm, about the maximum allowable for useful linear or non-linear optical integrated devices.

In this paper we report a major advance in planar tellurite waveguide fabrication using reactively sputtered films and a new reactive ion etch process to realize waveguides with minimum losses below even 0.1dB/cm for the first time. We also demonstrate strong nonlinear spectral broadening of 600fs optical pulses in excellent agreement with simulations.

2. Planar waveguide fabrication

Pure TeO_2 films were deposited using reactive sputtering of Tellurium metal in an Argon/Oxygen mixture in a manner similar to that of Nayak [30]. Deposition conditions were extensively investigated and an operating point chosen to yield stoichiometric TeO_2 films with high refractive index at 1550nm, where the stoichiometry was measured using energy dispersive X-ray analysis. Film refractive indices and dispersion were also measured on a 450-1650nm dual angle spectroscopic reflectometer (SCI Filmtek 4000) across a broad range of compositions. Propagation loss <0.1dB/cm was demonstrated in as deposited stoichiometric films at 1550nm as shown in Fig. 1, as determined from prism coupling experiments where the ~6cm light streak was captured with an InGaAs camera and processed to yield propagation loss.

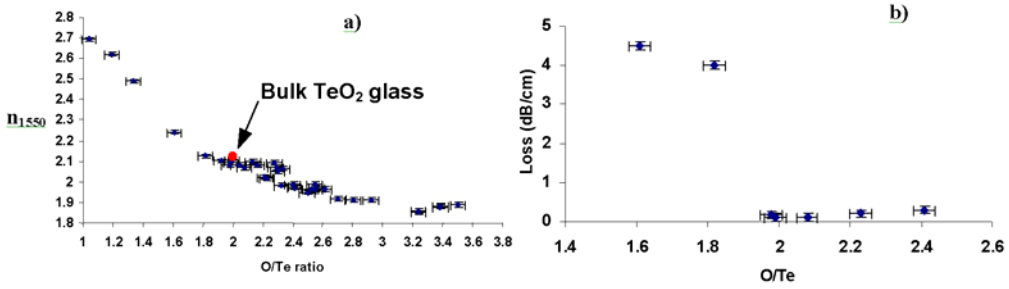

Fig. 1. a) Refractive index vs composition for sputtered TeO_2 films. The red dot indicates the value for bulk amorphous TeO_2. b) Propagation loss vs film composition measured from prism coupling light streaks in 8cm long samples.

A full DOE study revealed that the optimum sputtering conditions for the stoichiometric state were a pressure of 5mTorr, an Oxygen flow of 6.4sccm, an Argon flow of 8.6sccm, and an RF power of 150W. Films were deposited at 1.8µm thickness on <100> oriented 100mm silicon wafers with 2µm of thermal oxide as a bottom cladding. The refractive index of the as deposited films was measured at 2.08 (within 0.03 of the published index of bulk amorphous TeO_2) at 1550nm. Note that there is some uncertainty in the bulk value due to the difficulties in preparing amorphous TeO_2 samples without crystallization. Observation of the films using dark field microscopy and AFM revealed a smooth surface with a small number (~10/cm^2) of particles. An etch mask was then patterned using standard I-line contact photolithography methods utilizing 0.9µm thick Clariant AZ 701 MiR photoresist and 150nm thick Brewer Science XHRiC-16 bottom anti reflective coating (BARC). In addition to its lithographic function, the BARC layer also serves as a protective layer during the photoresist development process and isolates the Tellurite film from the aqueous base photoresist developer. This is crucial in avoiding damage to the tellurite film, where attack by common aqueous based chemistry was observed [29]. Nominal waveguide widths were 4µm. Special attention was paid to mask fabrication, the photo-mask having a measured line edge roughness <6nm RMS in a spatial wavelength range of 0.6-62µm (Taiwan Mask Corporation).

The waveguide ribs themselves were then exposed by room temperature reactive ion etching in an Oxford Instruments 80 series parallel plate system with 13.85MHz excitation. An all new etching process using an $H_2/CH_4/Ar$ gas mixture was developed to give the best results, as Tellurium Hydride is known to be volatile at room temperature in contrast to the halogen compounds of Tellurium which are not. Etch conditions were carefully optimized to

#114691 - $15.00 USD Received 23 Jul 2009; revised 8 Sep 2009; accepted 9 Sep 2009; published 17 Sep 2009

yield smooth almost vertical sidewalls as shown in Fig. 2., and far higher quality etching achieved compared to the purely physical sputter etching demonstrated previously which exhibited a high 5.7dB waveguide propagation loss at 1550nm [29].

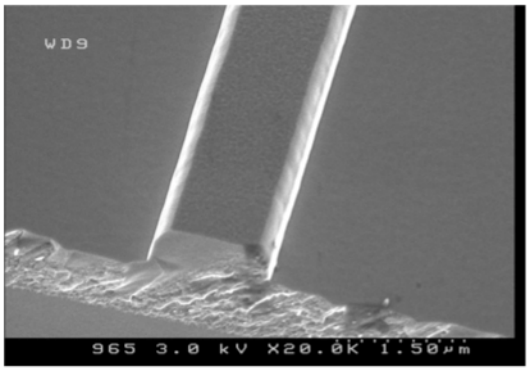

Fig. 2. Electron micrograph of etched TeO_2 rib structure

The final etching conditions were 30sccm H_2, 5sccm CH_4, 30sccm Ar, 30mT pressure, 150W RF power, and the rib was etched 0.8 microns deep. Post etch resist removal was accomplished by an oxygen plasma strip to avoid damaging the TeO_2 surface [29]. The waveguides were then clad with a 15µm thick film of UV cured inorganic polymer glass (RPO Pty Ltd, IPG) which has a refractive index of 1.509 at 1550nm. End facets were then hand cleaved on the waveguides with a diamond scriber. The resulting waveguide chips were 7.8cm long. Figure 3 shows the end facet of a finished waveguide.

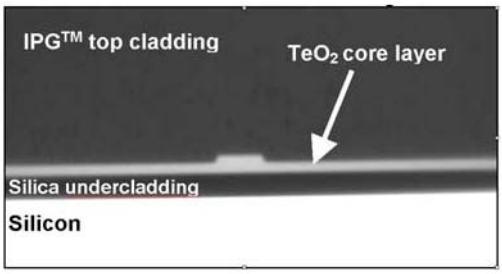

Fig. 3. Optical micrograph of cleaved finished waveguide in the 1.6 µm thick Tellurite film.

3. Linear characterization

Fiber coupling to the waveguide chips was accomplished using AR coated tapered lens fibers with a 2.5µm $1/e^2$ mode field diameter at 1550nm to suppress the Fabry-Perot cavity between the waveguide and fiber end faces. Modeling of the 4 micron waveguides used here with the full vector generic finite difference mode of the C2V Olympios software resulted in the modal fields shown in Fig. 4, and a calculated overlap loss to the fiber lens of 0.69dB (TE) and 0.79dB (TM) per end at 1550nm.

#114691 - $15.00 USD Received 23 Jul 2009; revised 8 Sep 2009; accepted 9 Sep 2009; published 17 Sep 2009

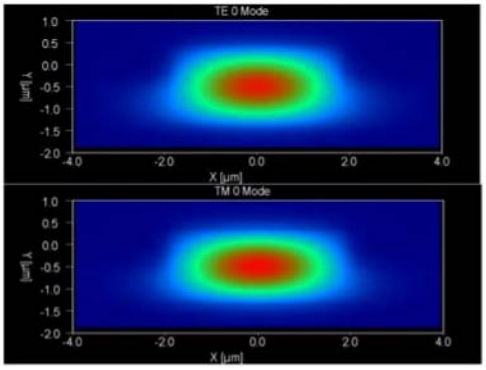

Fig. 4. Calculated mode intensity profiles for fabricated waveguide.

The 1550nm effective mode-field areas were calculated giving values of 4.0μm^2 and 3.7μm^2 for the TE and TM modes, respectively. For these waveguides the nonlinear parameter γ is ≈1 /W/m assuming the generally accepted nonlinear index of TeO_2 glass at about 25x silica [2]. The total dispersion of the waveguide was calculated at 60ps^2/km for the TE mode at 1550 nm, and 20ps^2/km for the TM mode.

Insertion loss measurements were made with either an external cavity laser based system or a fiber coupled mercury arc lamp based white light source/optical spectrum analyzer system. With the laser system, to avoid the insertion loss uncertainties from Fabry-Perot effects within the waveguide chip itself, an external cavity tunable laser with linewidth broadened to >7 times the minimum free spectral range of the waveguide chip was used as a source for measurements at 1550nm. Polarization dependent loss (PDL) data was gathered using a scanning polarization controller. In wideband measurements, the optical spectrum analyzer a 10nm resolution bandwidth was used to smooth out the chip Fabry-Perot resonances.

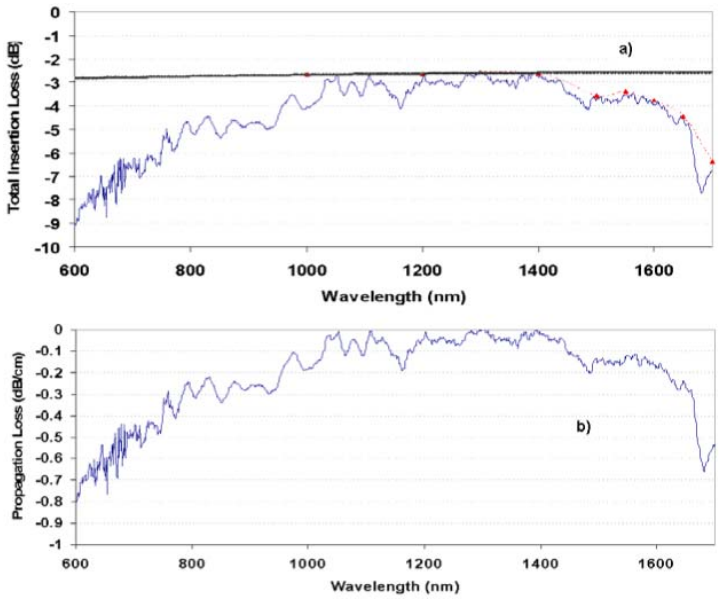

Fig. 5. a) Measured wideband fiber to fiber insertion loss for 7.8cm long 4μm wide TeO_2 waveguide. Solid curve indicates all calculated coupling and reflective losses as described in the text. Dashed curve shows fitted data points for absorption loss including Fabry-Perot enhancement as described in text b) Raw propagation loss after subtraction of calculated coupling and reflective losses and length normalization

#114691 - $15.00 USD Received 23 Jul 2009; revised 8 Sep 2009; accepted 9 Sep 2009; published 17 Sep 2009

Figure 5a shows the insertion loss data after normalization through the lensed fibers for a typical 4μm wide waveguide of 7.8cm length from 600 to 1700nm measured with the arc lamp source. Normalization spectra were recorded before and after the measurement to ensure the elimination of source drift, and there was a measurement uncertainty of about 0.3dB from FC fiber connector insertion repeatability induced during the alignment procedures.

The minimum observed insertion loss in Fig. 5a was 2.52dB including all coupling, overlap, and reflective losses, and the insertion loss at 1550nm was 3.51dB. The laser based measurement verified that from the OSA at 1550nm to within 0.05dB. The solid curve in Fig. 5a is a parabolic fit to the sum of the overlap losses and the average value of the Fabry-Perot Airy function, all calculated at 1000, 1200, 1550, and 1700nm and averaged over both polarization states. The overlaps and mode profiles were calculated using the full vector finite difference mode of C2V Olympios with the data for spot size variation of the tapered fiber lens provided by the manufacturer and the measured refractive index dispersion of the actual tellurite film and top cladding used to fabricate the waveguides. The Fabry-Perot average transmission was derived from facet reflectivities calculated using a plane wave decomposition method from the computed mode fields and effective indices [31].

Inspection of the calculated raw propagation losses shown in Fig. 5b suggest that the propagation losses across much of the 1000-1450nm window are 0.05dB/cm or less, more than an order of magnitude better than the best previously reported results [24] and a two order of magnitude improvement over the best prior plasma etched waveguides [29]. The connector induced measurement uncertainty corresponds to a propagation loss uncertainty of ~0.04dB/cm and is of the same order as the total measured propagation losses at the lowest loss points and therefore prevents the derivation of an accurate loss figure. However it is clear that the losses are very low indeed. The non flat nature of the response is we believe attributable to mode coupling and mode beating phenomena which generate wavelength dependent coupling effects as the waveguides support 3 modes at 1550nm (more at shorter wavelengths) and the input fibers become multimode below ~1250nm. Measured PDL for the waveguides was 0.35dB total at 1550nm including a measurement system PDL of 0.13dB, which compares favorably with the predicted ~0.2dB PDL from mode overlap losses noted above.

Also clear from Fig. 5 are that there are some absorption dips in the spectrum; one centered at 1166nm, one band from 1450nm to about 1610nm, and one strong dip centered at 1680nm. The 1680nm dip is related to strong C-H overtone absorption in the top IPG^{TM} cladding of the waveguide, and the other two bands likely result from OH absorption in the tellurite film, we believe as a result of the etch process. The exact nature and removal of these OH based absorptions is the subject of on going study, but they are clearly not seriously detrimental. In the raw data, the effects of absorption are influenced by the cavity effects and the actual absorption losses can be estimated by putting cavity loss into the Fabry-Perot response function. The dashed line and data points in Fig. 5a indicate such fitting from which the total propagation losses (of which absorption is dominant in this range) in Table 1 were derived:

Table 1 - Estimated absorption losses in the 1500-1700nm range

Wavelength (nm)	Loss (dB/cm)
1700	0.50
1650	0.24
1600	0.15
1550	0.10
1500	0.12

4. Nonlinear pulse propagation

To characterize the nonlinear properties of the waveguides we observed the nonlinear spectral broadening of pulses propagating through the 4μm wide waveguides. Pulses of ~1ps duration

#114691 - $15.00 USD Received 23 Jul 2009; revised 8 Sep 2009; accepted 9 Sep 2009; published 17 Sep 2009

at a 10MHz repetition rate were generated using a passively mode-locked fiber laser and launched into a tapered fiber lens pigtail 1m long containing a coiled loop polarization controller. The input power to the waveguide was varied by backing the launch fiber away from optimum focus, and the polarization controller was used to set the input to the desired polarization mode in conjunction with an imaging system, bulk polarizer and NIR InGaAs camera inspecting the output mode.

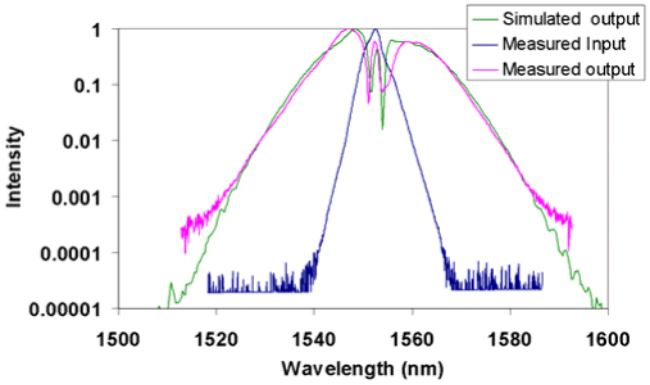

Fig. 7. Spectral broadening of pulses inside waveguide compared with results from Split Step Fourier modeling of waveguide with measured input pulse with n_2 varied to obtain best fit.

Figure 7 shows the experimentally observed self phase modulation broadening of the pulses resulting in 3 spectral lobes for an average power 0.9mW or a peak power of 110W inside the waveguide. No nonlinear absorption (i.e. two photon absorption) or optical damage was observed at the maximum fluence of 3GW/cm^2. The pulse exiting the launch fiber lens was characterized by Frequency Resolved Optical Gating-FROG (Southern Photonics HR150) with the waveguide chip removed and the receiving lens backed away to reduce the collected power ~20dB thereby avoiding nonlinear effects beyond the tip of the launch fiber. The pulse was found to be compressed to ~660fs in the launch pigtail. Agreement with the spectrum recovered from the FROG data was very good for both the launched pulse and the pulse at the end of the waveguide. Also plotted in Fig. 7 are the results from simulations solving the nonlinear Schrödinger equation by the split-step Fourier method using the measured input pulse and parameters based on the experimental setup and waveguide modeling described above, with $n_2 = 0.65 \times 10^{-20}\text{m}^2\text{W}^{-1}$. Good agreement with the experimental data is obtained confirming the nonlinear index of the deposited tellurite film at 25x silica as bulk glass [2].

5. Summary

Using a newly developed Hydrogen active species reactive ion etch process, TeO_2 planar rib waveguides with bulk like characteristics and minimum losses likely below 0.05 dB/cm were demonstrated, the lowest ever reported by a factor exceeding 10× . The suitability of these waveguides for all-optical signal processing is demonstrated by spectral broadening of sub-picosecond duration pulses, in excellent agreement with theory. Exploiting the low losses demonstrated in this paper with suitable zero dispersion waveguide designs and tellurite glasses with higher nonlinearity (e.g. 2-3x the measured value is possible [1,8]), a peak operating power for all-optical signal processing of ~1W appears reachable in integrated tellurite waveguide devices.

Acknowledgement

The support of the Australian Research Council through its Discovery grant program is gratefully acknowledged.

#114691 - $15.00 USD Received 23 Jul 2009; revised 8 Sep 2009; accepted 9 Sep 2009; published 17 Sep 2009